



THE UNIVERSITY *of* EDINBURGH

Edinburgh Research Explorer

Changes in temperature and heat waves over Africa using observational and reanalysis data sets

Citation for published version:

Engdaw, MM, Ballinger, AP, Hegerl, GC & Steiner, AK 2022, 'Changes in temperature and heat waves over Africa using observational and reanalysis data sets', *International Journal of Climatology*, vol. 42, no. 2, pp. 1165-1180. <https://doi.org/10.1002/joc.7295>

Digital Object Identifier (DOI):

[10.1002/joc.7295](https://doi.org/10.1002/joc.7295)

Link:

[Link to publication record in Edinburgh Research Explorer](#)

Document Version:

Publisher's PDF, also known as Version of record

Published In:

International Journal of Climatology

Publisher Rights Statement:

© 2021 The Authors. International Journal of Climatology published by John Wiley & Sons Ltd on behalf of Royal Meteorological Society

General rights



Copyright for the publications made accessible via the Edinburgh Research Explorer is retained by the author(s) and / or other copyright owners and it is a condition of accessing these publications that users recognise and abide by the legal requirements associated with these rights.

Take down policy

The University of Edinburgh has made every reasonable effort to ensure that Edinburgh Research Explorer content complies with UK legislation. If you believe that the public display of this file breaches copyright please contact openaccess@ed.ac.uk providing details, and we will remove access to the work immediately and investigate your claim.



Changes in temperature and heat waves over Africa using observational and reanalysis data sets

Mastawesha Misganaw Engdaw^{1,2}  | Andrew P. Ballinger³  |
Gabriele C. Hegerl³  | Andrea K. Steiner^{1,4} 

¹Wegener Center for Climate and Global Change (WEGC), University of Graz, Graz, Austria

²FWF-DK Climate Change, University of Graz, Graz, Austria

³School of Geosciences, University of Edinburgh, Edinburgh, UK

⁴Institute for Geophysics, Astrophysics and Meteorology/Institute of Physics, University of Graz, Graz, Austria

Correspondence

Mastawesha Misganaw Engdaw, Wegener Center for Climate and Global Change (WEGC), and FWF-DK Climate Change, University of Graz, Graz, Austria.
Email: mastawesha.engdaw@uni-graz.at

Funding information

Austrian Science Fund, Grant/Award Number: W1256

Abstract

Providing comprehensive regional- and local-scale information on changes observed in the climate system plays a vital role in planning effective and efficient climate change adaptation options, specifically over resource-limited regions. Here, we assess changes in temperature and heat waves over different regions of the African continent, with a focus on spatiotemporal trends and the time of emergence of change in hot extremes from natural variability. We analyse absolute and relative threshold indices. Data sets include temperatures from observations (CRUTS4.03 and BEST) and from three representative state-of-the-art reanalyses (ERA5, MERRA2 and JRA-55) for the common period 1980–2018. Statistically significant warming is observed over all regions of Africa in temperature time series from CRU observations and reanalysis data, although the trend strength varies between data sets. Also, extreme temperatures and heat wave indices from BEST observations and all reanalysis data sets reveal increasing trends over all regions of the African continent. However, there are differences in both trend strength and time evolution of heat wave indices between different reanalysis data sets. Most data sets agree in identifying 2010 as a peak heat year over Northern and Western Africa while Eastern and Southern Africa experienced the highest heat wave occurrence in 2016. Our results clearly reveal that heat wave occurrences have emerged from natural climate variability in Africa. The earliest time of emergence takes place in the Northern Africa region in the early 2000s while in the other African regions emergence over natural variability is found mainly after 2010. This also depends on the respective index metrics, where indices based on more consecutive days show later emergence of heat wave trends. Overall, significant warming and an increase in heat wave occurrence is found in all regions of Africa and has emerged from natural variability in the past one or two decades.

KEYWORDS

Africa, climate change, heat waves, observations, reanalysis, temperature extremes, time of emergence

1 | INTRODUCTION

The Earth's climate system is warming unequivocally, largely due to human influences (IPCC, 2014). Anthropogenic climate change alters the temperature distribution in terms of variability and mean, which further causes changes in temperature extremes and heat waves. In addition to temperature, also humidity, wind and incident radiation play a role in altering the occurrence and characteristics of heat waves (Russo et al., 2017; Sherwood, 2018; Llargeron et al., 2020; Li et al., 2020). The occurrence and intensity of heat waves has changed since the 1950s (Seneviratne et al., 2012), reported for different parts of the world (Kuglitsch et al., 2010; Smith et al., 2013; Cowan et al., 2014; Rohini et al., 2016; Liao et al., 2018), as well as their duration and spatial extent (Oueslati et al., 2017), specifically impacting Africa.

Anthropogenic driven warming often manifests its damaging effects through weather- and climate-related temperature extremes. Heat waves are one of the deadliest natural disasters. Increase in intensity and frequency of heat wave events contribute to loss of human lives and crop damages. Heat waves lead to large socioeconomic impacts comprising agriculture, infrastructure, energy consumption and supply and other sectors (Lobell et al., 2011; Coumou and Rahmstorf, 2012; Chapman et al., 2013; Perkins, 2015). Heat waves impact human health and increase morbidity and mortality of people, especially the most vulnerable population. In the years between 1999 and 2009, 11,000 excess hospitalizations were reported due to extreme heat in California (Guirguis et al., 2014), whereas the 2003 European heat wave caused up to 70,000 deaths (Robine et al., 2008). The 2015 India-Pakistan heat wave caused around 2,500 and 700 deaths in India and Pakistan, respectively (Masood et al., 2015; Ratnam et al., 2016). Russia's 2010 heat wave caused around 15,000 deaths together with an estimated economic damage of around 15 billion USD (Lau and Kim, 2012).

Despite its relatively small contribution to global warming emissions, Africa is among the developing regions that are facing disproportionately greater impacts from climate-related extremes and is in the climate zone where the temperature change signal is expected to emerge first from climate variability (e.g., Mahlstein et al., 2011). Africa's higher exposure to the impacts of climate change arises from its increased vulnerability due to limited adaptation and economic capacity, and ineffective institutional structure. Consequently, the resulting societal impacts of heat waves, both during and after the events are expected to be much higher in Africa (IPCC, 2014). In the last three decades, Africa has suffered 27% of the global fatalities due to climate

and weather-related extremes (Munich Re, 2011). Furthermore, the droughts of 1974–1975 (over the Sahel region) and 1984–1985 (over Sudan and Ethiopia) alone led to the death of hundreds of thousands of people (Guha-Sapir et al., 2004). Urbanization and fast-growing population pressure on land use and land cover further exacerbates the vulnerability of the region to heat island effects and heat waves.

Many regions of Africa have already experienced increases in surface temperature as reported for different subregions, analysing various data sets. Temperatures are estimated to be 1–2°C higher in the recent decades than during the Medieval Climate Anomaly (Nicholson et al., 2013). Maximum and minimum temperatures also showed an increasing trend over Ethiopia, Kenya and Tanzania (Gebrechorkos et al., 2019). However, both maximum and minimum temperatures show higher variability over Ethiopia. Ceccherini et al. (2017) reported an increase in the spatial coverage of maximum temperature from 37.3% during the period 1981–2005 to 60.1% during the period 2006–2015 of Africa's terrestrial surface area.

While Russo et al. (2016) showed the occurrence of more intense heat waves with longer duration and wider extent in recent years in Africa, Vizy and Cook (2012) estimated an increase of 40–60 heat wave days per year on average in the period 1989–2009 over Northwestern Sahara. Furthermore, the significant increase in temperature, specifically during warm seasons, over Northern Africa is unlikely to be due to natural forcings alone (Barkhordarian et al., 2012, 2012). In addition to the ongoing socio-economic challenges throughout the continent, changes in temperature and heat waves are expected to increase energy costs in the future. Parkes et al. (2019) estimated Africa's cost of energy-intensive cooling systems to be 51 billion USD and 487 billion USD by 2035 and 2076, respectively. As indicated by The World Bank Group (2020) only 44.5% of the Sub-Saharan population has access to electricity. Therefore, such an increase in energy costs would likely be initially accompanied by lower access to electricity across the continent. The increasing demand for currently unavailable, insufficient and/or unaffordable electricity for ventilation will exert additional pressure on the least developed subregions of the continent.

Improving knowledge of temperature changes, the occurrence of heat waves, and the time of emergence over natural variability has vital societal importance (Harrington et al., 2016). Identifying the time when the signal of anthropogenic climate change begins to distinctly emerge from the background natural variability is important for climate change predictions and risk assessment (Hawkins and Sutton, 2012; Lehner et al., 2017), and for designing adaptation strategies (Hawkins

et al., 2014). Several studies have assessed changes in heat waves over Africa; in the Sahel region (Oueslati et al., 2017), over Ethiopia, Kenya and Tanzania (Gebrechorkos et al., 2019), over northern tropical Africa (Moron et al., 2016), and at continental scale (Russo et al., 2016; Ceccherini et al., 2017). These studies showed that there is an increase in temperature and heat waves over different regions of Africa, and there may be an increase at continental scale. However, it is challenging to draw comprehensive regional information for climate change adaptation and mitigation as well as for litigation from such fragmented studies.

In this study, we provide a systematic assessment of temperature changes based on two observational and three reanalysis data sets for the African continent. We analyse the change in extreme temperatures and heat waves across different African regions. For the first time, we assess the emergence of heat waves over natural climate variability based on reliable and robust indicators of extremes from multiple observation-based state-of-the-art data sets. This gives a picture of changes across climatologically different African regions. Using a set of indicators, we also demonstrate the influence of several heat metrics definitions (i.e., different thresholds and duration requirements) on the time of emergence of heat wave occurrence from natural variability.

2 | DATA AND METHODS

2.1 | Temperature data sets

Observational and reanalysis data sets of 2 m air temperature were used in this study, over the common time period 1980–2018. We used observations from the Climate Research Unit (CRU) Time Series (TS) version 4.03 (CRU TS4.03), provided as monthly time series at a spatial resolution of $0.5^\circ \times 0.5^\circ$, denoted as CRU in the following. In addition, the Berkeley Earth Surface Temperature (BEST) observational data set was used, where daily minimum and maximum temperatures are available at a spatial resolution of $1^\circ \times 1^\circ$ in longitude and latitude. Daily temperature data and monthly mean data were used from the following reanalyses: the European Centre for Medium-Range Weather Forecasts Reanalysis 5 (ERA5; Hersbach et al., 2020), National Oceanic Atmospheric Administration's Modern-Era Retrospective Analysis for Research and Applications, Version 2 (MERRA2; Gelaro et al., 2017), and Japanese Meteorological Agency's 55-year reanalysis (JRA-55; Kobayashi et al., 2015). These data sets comprise the only presently available observational data set covering

the African continent at daily resolution and the three most recently published and state-of-art reanalysis data sets, which are regarded representative for this study. We use these different data sources to assess the robustness of trends and variability analysed here, as reanalyses differ in model and data streams used, and observational products in data processing. We consider all data products a priori equally likely. Exceptions are cases of known problems (e.g., see Section 3.2 below discussion of issues in tropical Africa for MERRA2), and we would like to flag the limited coverage by station data for BEST and CRU.

We computed daily maximum and daily minimum temperatures from ERA5 hourly data while maximum and minimum temperatures were available at daily temporal scale for MERRA2 and JRA-55. Monthly mean temperatures were available and downloaded for CRU and ERA5. For MERRA2 and JRA-55 we averaged daily temperatures to monthly means. The horizontal spatial resolution for ERA5, MERRA2 and JRA-55 is $0.25^\circ \times 0.25^\circ$, $0.625^\circ \times 0.5^\circ$ and $1.25^\circ \times 1.25^\circ$ in longitude and latitude, respectively.

The data sets are available from the following weblinks. The CRUTSv4.03 data were downloaded from the Natural Environment Research Council's Data Repository for Atmospheric Science and Earth Observation (UK) at <http://archive.ceda.ac.uk/>. BEST data set is obtained from <http://berkeleyearth.org/data-new/>. The ERA5 data were downloaded from <https://cds.climate.copernicus.eu/cdsapp#!/home>. MERRA2 is available at <https://disc.gsfc.nasa.gov/datasets?keywords=%22MERRA-2%22&page=1&source=Models%2FAnalyses%20MERRA-2>, and JRA-55 at https://jra.kishou.go.jp/JRA-55/index_en.html.

We used monthly temperature to assess long-term temperature changes and their representation in CRU observations and the reanalyses. Changes in temperature extremes and heat waves were assessed from daily temporal-scale temperatures of observational BEST and the reanalysis data sets. Temperature anomalies were computed for each data set relative to the reference period 1980–2009. Decadal trends and associated 95% confidence intervals in monthly mean temperature anomalies were computed based on ordinary linear regression. We assessed changes in monthly mean temperature and extremes over the African continent and for four large-scale regions defined after Field et al. (2012): Northern Africa (NA), Western Africa (WA), Eastern Africa (EA) and Southern Africa (SA), all shown in Figure 1. Area weighting (by the cosine of the latitude) was applied for computation of the large-scale regions.

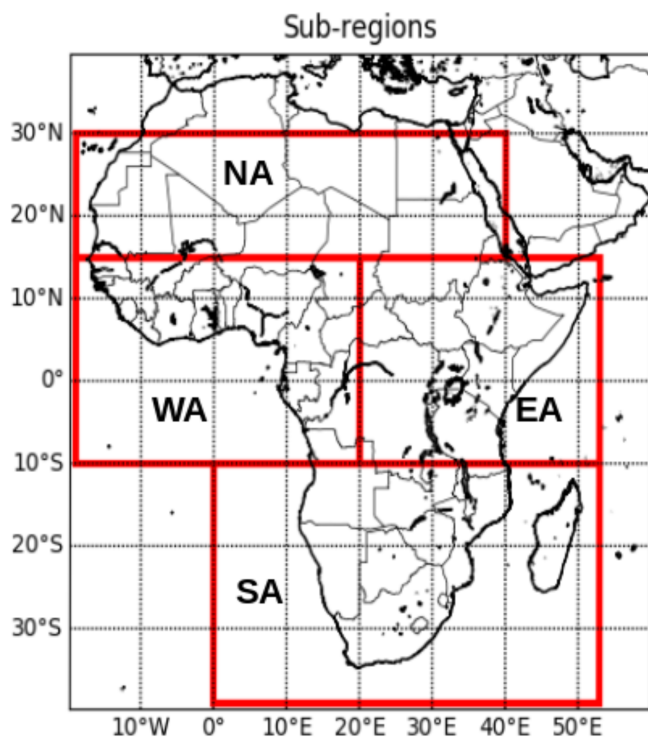


FIGURE 1 Sub-regions over the African continent used in this study, Northern Africa (NA), Western Africa (WA), Southern Africa (SA) and Eastern Africa (EA), defined after Field et al. (2012) [Colour figure can be viewed at wileyonlinelibrary.com]

2.2 | Definitions of heat wave indices

Climate extremes, in general, can be defined by their rare occurrence and/or the high magnitude of damages to society and ecosystems (Hegerl et al., 2011). Specifically, heat waves are usually defined as consecutive days of extremely hot temperatures which exceed thresholds of temperature and span consecutive days (Wang et al., 2019). A number of factors affect a heat wave's definition, including the sectors (health, infrastructure, agriculture) that might be of particular interest, hence different characterizations of extreme heat are often targeted to particular impacts. What can be described as a heat wave also varies by geographic and climatic conditions. Consequently, there is no single and universally accepted definition (Oueslati et al., 2017; Shafiei Shiva et al., 2019). Differing thresholds, duration and ancillary variables contribute to divergence in defining heat waves (Smith et al., 2013).

In assessing the changes in heat waves in this study, we use indices introduced by the Expert Team on Climate Change Detection, Monitoring and Indices (ETCCDI; <http://etccdi.pacificclimate.org/>), defined in Table 1. Summer days (SU), the percentage of days above the 90th percentile (TX90P) and warm spell duration

TABLE 1 ETCCDI indices of temperature extremes used in this study

Abbreviation	Description of indices
SU	Number of summer days: Maximum temperature (T_{\max}) > 35°C
TR	Number of tropical nights: Minimum temperature (T_{\min}) > 24°C
TX90P	Percentage of days when T_{\max} >90th percentile
WN	Number of warm nights when T_{\min} >95th percentile for at least two consecutive days
WSDI_3	Warm spell duration index (annual count of days) when T_{\max} >95th percentile for at least three consecutive days
WSDI_6	Warm spell duration index (annual count of days) when T_{\max} >90th percentile for at least six consecutive days

index (WSDI) are computed from daily maximum temperature, whereas tropical nights (TR) and warm nights (WN) are computed from daily minimum temperature. Furthermore, the indices used in this study can be grouped as absolute threshold (SU and TR) and relative threshold (TX90P, WN and WSDI) indices.

Using a subset of years as the reference period is a typical approach when calculating thresholds for percentile-based indices (Christidis and Stott, 2016; Guo et al., 2017). However, using a subset of years to compute thresholds can cause differences in exceedances between the years within the reference period and years outside the reference period (Zhang et al., 2005). Exceedances computed for years outside the reference period, for temperature, can become higher than exceedances computed for years used in the reference period. To avoid this inconsistency, in this study, we use the whole period of analysis (1980–2018) to compute thresholds of percentile-based indices in order to avoid jumps in exceedances per year along the years of analysis. Thresholds are then smoothed over adjacent days to reduce noise and improve robustness. As demonstrated by Zhang et al. (2005), a narrow smoothing window (5 days) can result in biases of exceedance rates due to uncertainty in estimating percentile thresholds, while a wide smoothing window (25 days) can reduce the amplitude and annual cycle of thresholds, particularly in regions with complex seasonal cycle. In this study, we use a moderate smoothing window of 15 days to allow for robust thresholds while still capturing the seasonal cycle of thresholds. Combining such moderate smoothing with a reference period computed over the entire time series ensures a

homogenous and robust estimate of exceedance rates across the different African regions from observational and reanalysis data.

Ordinary linear regression, accounting for autocorrelation, is used to compute decadal trends of monthly mean temperature time series and decadal trends of extreme temperatures and heat wave indices. Mann-Kendall's significance test is used to assess the significance of change in heat wave indices, at regional scale (over the four large regions NA, WA, EA and SA), and at local scales (on the longitude-latitude grid).

2.3 | Time of emergence of heat waves

Time of Emergence (ToE) is the time at which the signal of heat wave indices begins to emerge above, and then continuously exceeds the natural climate variability (noise). Because of less annual variability of temperature, heat waves show earlier time of emergence in tropical regions than in high latitudes (Diffenbaugh and Scherer, 2011; Mahlstein et al., 2011; King et al., 2017). The ToE of heat waves is identified using the signal-to-ratio method by Hawkins and Sutton (2012). We compute the signal using anomalies of heat wave indices of the respective data sets relative to the reference period. The noise is estimated using the standard deviation of de-trended anomalies of the indices in the reference period (1980–2009). The year of emergence of heat waves is determined as the year when the computed signal-to-noise ratio continuously stays above a specified threshold, which here is one standard deviation of de-trended noise. Using a threshold value higher than one would give greater confidence in the ToE of heat waves. However, the reference period, 1980–2009, is in the recent warming period, and does not reflect the supposed-quasi-natural climate variability of the regions. Therefore, we use one standard deviation as the threshold in identifying the ToE for the heat wave indices over the last nearly four decades.

For the preprocessing of the data sets, we used NetCDF Operator (Robine et al., 2008), available at <http://nco.sourceforge.net/nco.html>, to concatenate, permute dimensions, rename, and extract the African regions from the global data set. Climate Data Operator (CDO), available at <https://code.mpimet.mpg.de/projects/cdo>, was applied for additional preprocessing of time-series data. The number of heat wave days, which fulfil the respective definitions, were computed using CDO software. Python's `scipy.stats` package (<https://www.scipy.org/about.html>) was used for the statistical analyses.

3 | RESULTS AND DISCUSSION

3.1 | Changes in monthly mean temperature

Figure 2 shows the monthly temperature climatologies (1980–2018) of the four different African regions, computed from the CRU observations and the ERA5, MERRA2 and JRA-55 reanalysis data sets. The data sets show good agreement in climatological temperature. Because of the equatorial location of EA and WA regions, they show a relatively similar magnitude and pattern of the annual temperature cycle. However, WA shows higher variability and amplitude of the bimodal temperature patterns. The Northern- and Southern-hemispheric location of NA and SA regions clearly show the winter-summer seasonal contrast. The annual cycle and seasonality are most pronounced over NA and SA, with maximum and minimum temperatures, respectively, in July, while the equatorial climate over EA and WA shows a bimodal temperature pattern, with one maximum in March to April and a second maximum in September to October. Both the observational and reanalysis data sets are consistent in their representation of the annual cycle, with only small differences detected. Temperatures from CRU exceed those of the reanalysis data sets in the months from March to December over WA and EA, and from January to July over SA. While JRA-55 shows the highest temperature over NA in all months, MERRA2 shows the highest temperature in months from August to December over SA.

Figure 3 shows results of the trend analysis of monthly temperature anomalies (after the seasonal cycle is removed) for the period 1980–2018 from CRU, ERA5, MERRA2 and JRA-55 over the four African regions. Despite differences in the magnitudes of trends, all the data sets agree on increasing temperature trends over 1980–2018 and show significant warming in all of the regions. Overall, highest trends are found over NA with more than 0.25°C per decade (from $0.27 \pm 0.07^{\circ}\text{C}$ to $0.41 \pm 0.10^{\circ}\text{C}$) while trends are lowest over SA with about 0.15°C per decade (from $0.15 \pm 0.08^{\circ}\text{C}$ to $0.19 \pm 0.08^{\circ}\text{C}$). Observations from CRU show the largest trend over NA with $0.28 \pm 0.07^{\circ}\text{C}$ per decade while trends are $0.16 \pm 0.04^{\circ}\text{C}$ per decade over WA, $0.18 \pm 0.04^{\circ}\text{C}$ per decade over EA, and $0.17 \pm 0.04^{\circ}\text{C}$ per decade over SA. As shown by the larger error bars (95% confidence interval), the highest variability within the data sets is observed over NA, nevertheless the trends are all significant. The largest spread in trends (between data sets) is found over WA (error bars hardly overlap) while the lowest spread is in SA.

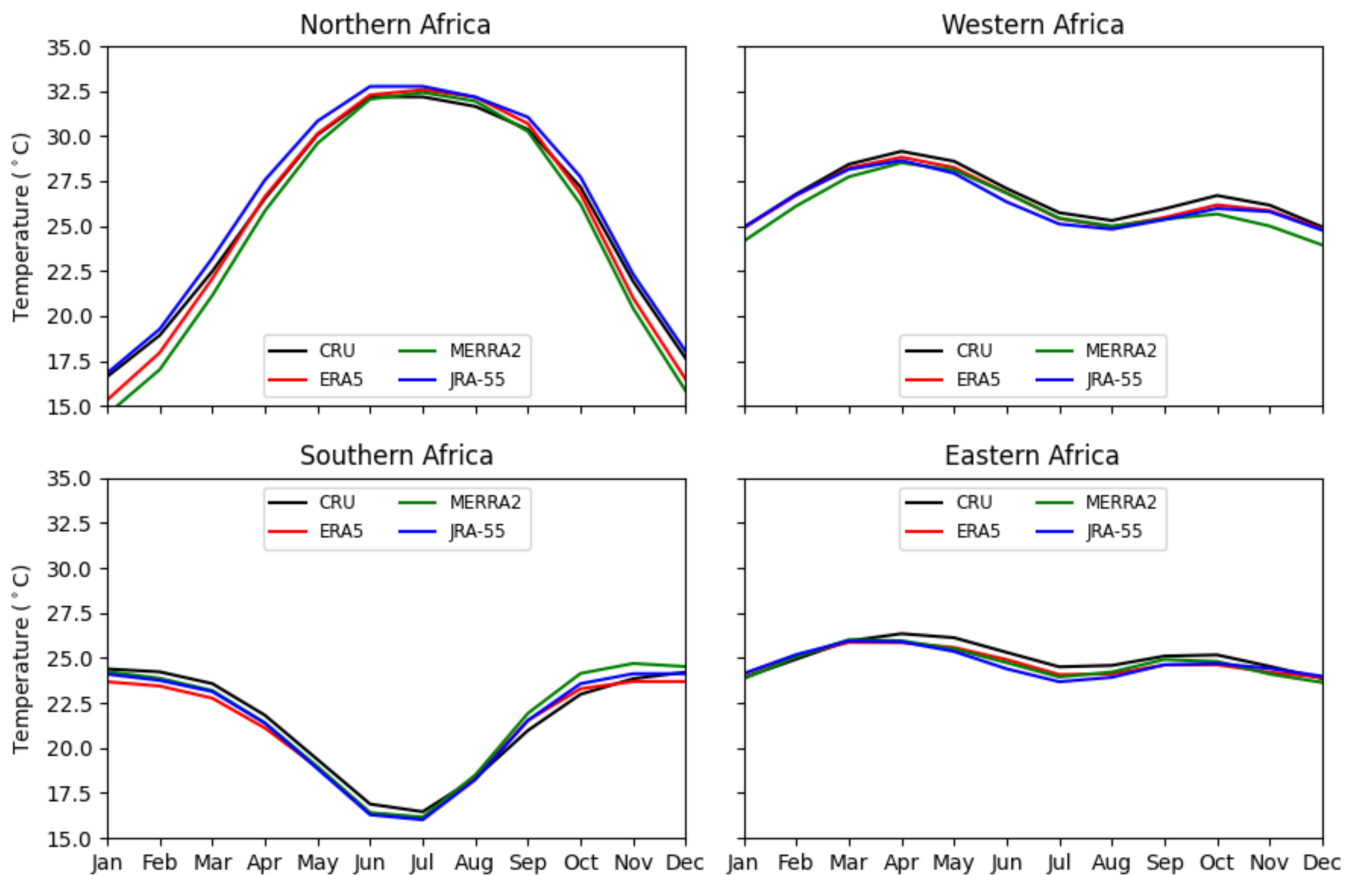


FIGURE 2 Monthly mean temperature climatology (1980–2018) of Northern Africa (NA), Western Africa (WA), Southern Africa (SA) and Eastern Africa (EA) using multiple datasets [Colour figure can be viewed at wileyonlinelibrary.com]

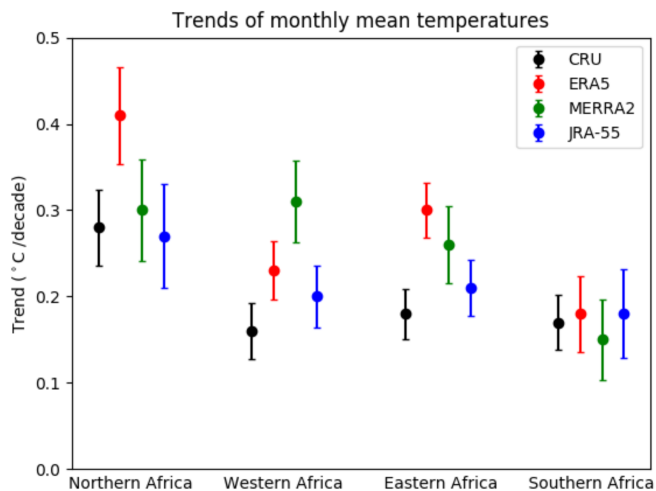


FIGURE 3 Trends of monthly mean temperature (1980–2018) from CRU, ERA5, MERRA2 and JRA-55 data sets over NA, WA, EA and SA regions. Error bars denote the 95% confidence interval of fitting decadal trends [Colour figure can be viewed at wileyonlinelibrary.com]

The greatest difference between trends in ERA5 and CRU is observed over NA and EA. JRA-55 shows consistent agreement with the observed CRU trends in all

regions. In most cases, the reanalysis data sets exhibit higher decadal trends than the CRU observations. However, good agreement is found between monthly temperature time series of reanalyses and of CRU observations from correlation analysis. Positive correlation coefficients show that the monthly time series of temperature anomaly (1980–2018) from all reanalysis data sets are in good agreement with the observed CRU time series. ERA5 monthly temperature shows the highest correlation with CRU temperature, with correlation coefficients being 0.95, 0.93, 0.86 and 0.82, over WA, NA, SA and EA regions, respectively. MERRA2 shows the lowest correlation with CRU, with coefficients of 0.78 and 0.75 over WA and EA, respectively, because of unreliably high temperatures between the years from 2000 to 2010 (discussed below).

3.2 | Changes in extreme temperatures and heat waves

Changes in extreme temperatures and in heat waves over 1980–2018 are presented in Figure 4 based on BEST observations and reanalyses. Time series of annual

maximum and minimum temperature anomalies (Figure 4, rows a and b) show an increasing trend in all African regions, consistently in all data sets. Extreme

daytime and nighttime temperatures (Figure 4, rows c and d) and heat wave indices (Figure 4, rows e to h) indicate changes in SU, TR, TX90P, WN, WSDI_3 and

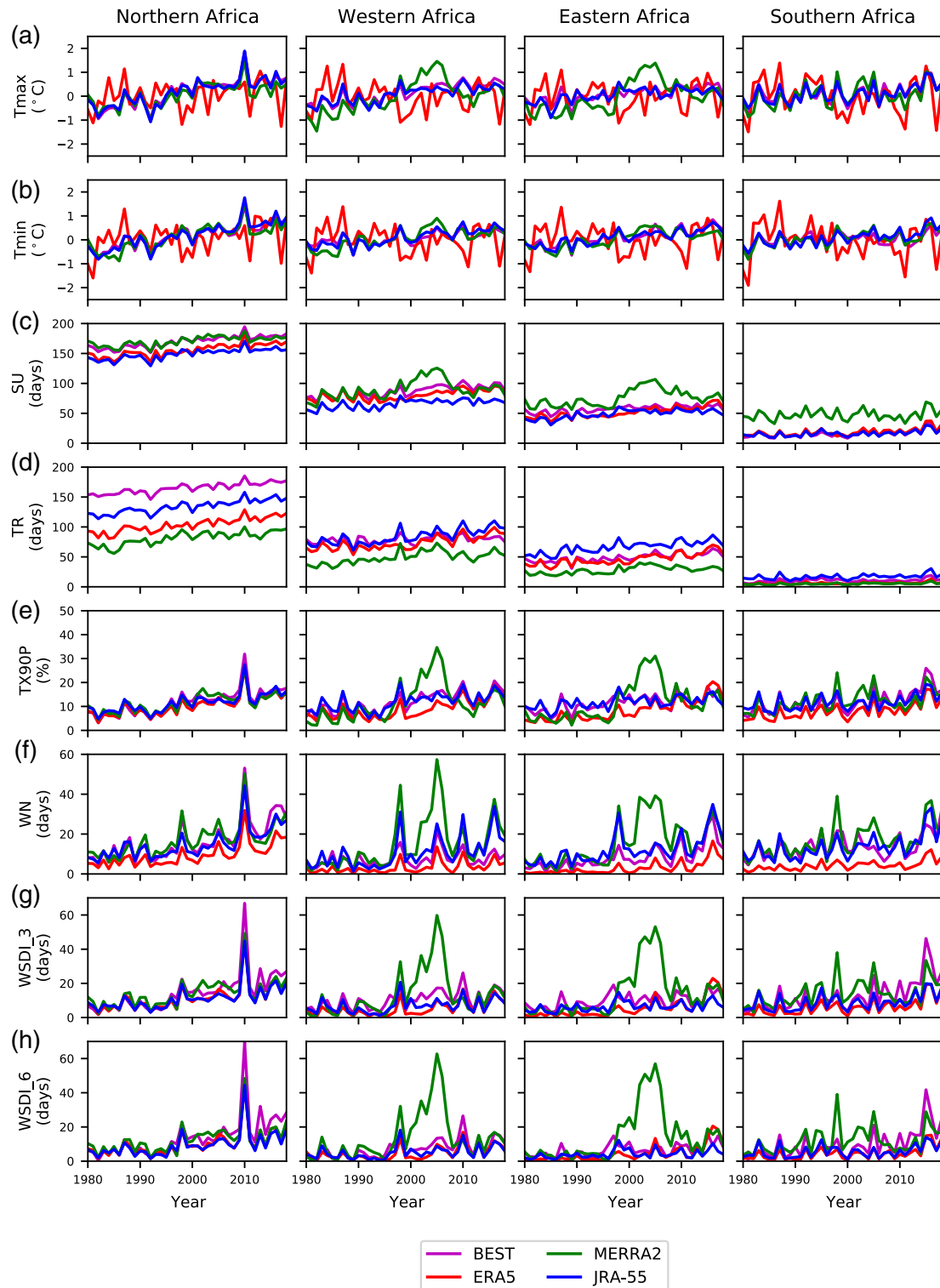


FIGURE 4 (a,b) Annually averaged daily maximum and minimum temperature anomalies (T_{max} and T_{min}), (c,d) number of summer days and tropical nights (SU and TR), and (e,h) heat wave indices (frequency of daily maximum temperature TX90P, number of warm nights WN, and number of days of 3-day and 6-day warm spells WSDI_3 and WSDI_6) shown for (left to right) the African regions NA, WA, EA and SA from observational BEST and reanalysis data sets (ERA5, MERRA2 and JRA-55) [Colour figure can be viewed at wileyonlinelibrary.com]

WSDI_6 over the African regions, based on daily maximum and minimum temperatures of BEST observations, and ERA5, MERRA2 and JRA-55 reanalysis data sets. All the indices show an increase in heat wave days over the African regions. As the climatology of the regions presented in Section 3.1 (see Figure 2) shows, NA and SA regions have the highest and the lowest seasonal cycles, respectively. Consequently, absolute-threshold-based indices, SU and TR, show the highest number of heat wave days per year over NA and the lowest number of heat wave days per year over SA. Because of the persistence requirement of two, three and six consecutive days for WN, WSDI_3 and WSDI_6 (Figure 4, rows f to h), respectively, the number of heat wave days per year in these indices is smaller than for indices based on absolute thresholds (SU and TR) or percentiles (TX90P). The data sets show good agreement in capturing both the magnitude and temporal evolution of heat waves. Over NA, the indices WN, WSDI_3 and WSDI_6 based on the observational BEST data set captured the highest number of heat wave days since the 2000s.

Noticeable is that MERRA2's annual maximum temperature anomaly shows exceptionally higher positive deviations over WA and EA regions between the years 2000 and 2010. Consequently, all MERRA2 indices computed from maximum temperature over WA and EA regions are much higher than those from the other data sets over the same regions and time period. The 2000s in MERRA2 are marked by increased variability and decrease in specific humidity from 850 hPa to the land surface. This led to biases in the middle and lower troposphere and is a deficiency transferred from the predecessor version of MERRA2 (Gelaro et al., 2017). Spatially, those biases are located over the tropical regions (20°S–20°N) where WA and EA regions are entirely contained. We further examined MERRA2's high heat wave occurrence and computed the difference in mean WSDI_6 between MERRA2 and ERA5 between 2000 and 2010. We found the biases reported by Gelaro et al. (Gelaro et al., 2017) located over the tropical mountainous regions of the Ethiopian highlands, WA and Equatorial Central Africa (not shown). However, TR from MERRA2 consistently shows the lowest number of heat wave occurrences in all regions. WN, WSDI_3 and WSDI_6 indices from MERRA2 show consistency in capturing high heat wave days in the well-known El Niño year (1997/98). All data sets agree in capturing high heat wave days in the year 1997/98 over all African regions, though with different magnitude. Indices from MERRA2 show the highest number of heat wave days in the year 1997/98 over WA and SA regions.

All data sets show that NA experienced an exceptionally high number of heat wave days in 2010. SU, TR,

TX90P, WSDI_3 and WSDI_6 indices computed from ERA5 identify 2010 as the year of highest heat wave days over WA. Furthermore, 2016 is identified (in TR TX90P, WSDI_3 and WSDI_6 metrics) as the year with the second highest number of heat wave days over WA as shown by ERA5 and JRA-55. In the EA and SA regions, 2016 was the year with the highest number of heat wave days as shown by most of the indices.

Even though there are differences in the number of heat wave days among the indices analysed from BEST, ERA5, MERRA2 and JRA-55 data sets, the heat wave indices consistently show an increasing number of heat wave days per year over the recent decades. Neglecting MERRA2's unreliably high number of heat wave days between the years 2000 and 2010 over WA, EA and SA, all of the indices from the remaining reanalysis data sets and the BEST observations agree on identifying 2010 (mainly over NA but also over WA) and 2016 (over EA and SA) as years with the highest number of heat wave days. Note that unlike 2016 (over EA and SA), 2010 (over NA) has an extraordinarily high number of heat wave days compared to the remaining years in the respective regions.

This is further demonstrated in Figure 5, which displays normalized histograms for TX90P for the period 1980–2018 based on ERA5. It clearly shows that the years 2010 (over NA) and 2016 (over EA, WA and SA) are at the far edge of the respective distribution underpinning that 2010 and 2016 were exceptionally warm years. Also, the years 2015, 2017 and 2018 contributed with a high number of extreme days in EA, WA or SA.

Largerón et al. (2020) investigated the April 2010 heat wave over Northern Africa. During that month, large areas of the Saharan desert and Sahel regions exceeded $T_{\max} > 40^{\circ}\text{C}$ and $T_{\min} > 27^{\circ}\text{C}$ for more than 5 consecutive days. Evan et al. (2015) reported that daily maximum temperature reached 44.5°C over Niamey. Radiation budget analysis showed that there was more incoming longwave radiation and less incoming shortwave radiation. Incoming shortwave anomalies were reduced due to enhanced cloud formation over the region while longwave radiation was enhanced due to the greenhouse effect of a larger amount of water vapour. Early northward transport of monsoon flow and tropical plumes were sources of water vapour for the Western Sahel and Sahara regions, respectively (Largerón et al., 2020). Thus, more emissivity of longwave radiation by the land surface and less cooling of the atmospheric surface layer led to night-long warming (Largerón et al., 2020). Consequently, the greenhouse effect of water vapour led to an increase in minimum temperatures over the Sahel region (Oueslati et al., 2017). The occurrence of the 2010 heat wave event had significant impacts on human health, hydrology and agriculture in the region (Evan et al., 2015).

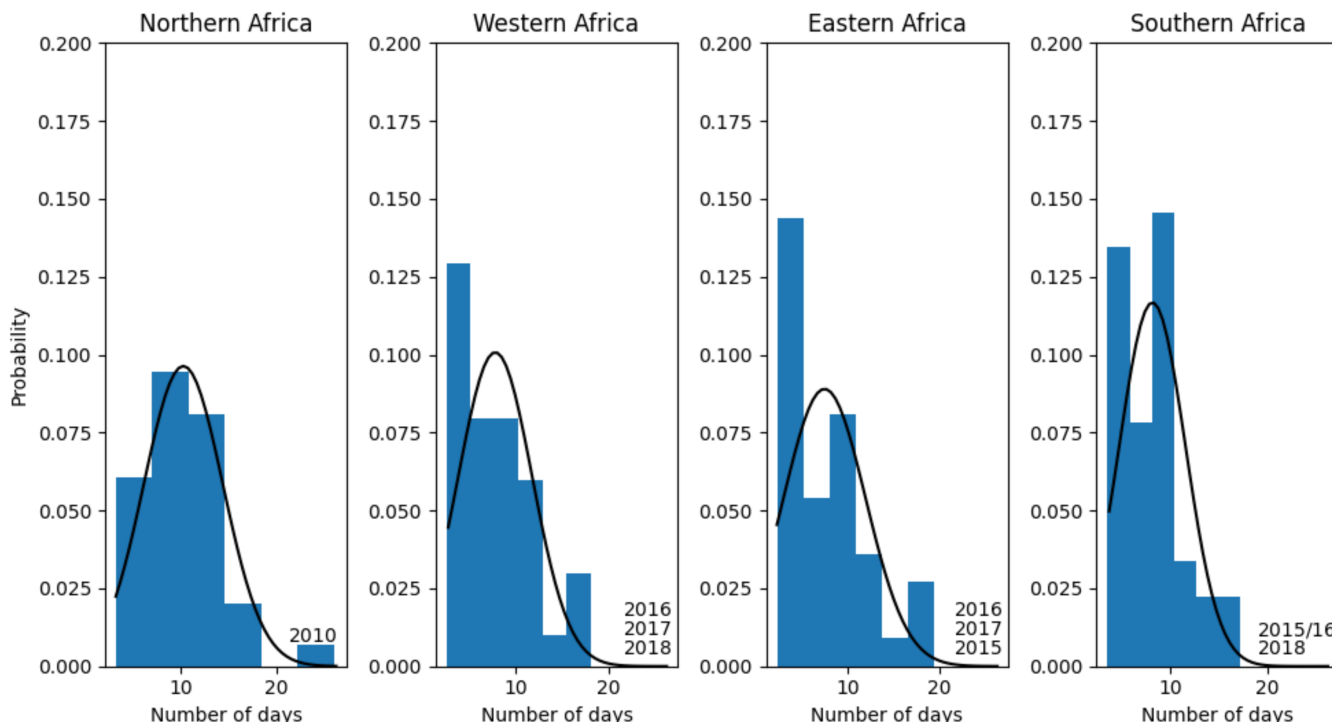


FIGURE 5 Normalized histograms of average exceedance values of TX90P (number of days) from ERA5 for (left to right) the African regions NA, WA, EA and SA. Numbers in tails indicate extreme years [Colour figure can be viewed at wileyonlinelibrary.com]

3.3 | Trends in heat wave indices

Our analysis reveals a consistently increasing trend in heat wave days per decade across all regions of the African continent as summarized in Figure 6. The highest and lowest decadal trends of both extreme temperatures and heat wave days are found in NA and SA regions, respectively. SU and TR, compared to the other indices, show the greatest change (per decade) in all regions, except in SA. In SA, the decadal trends for SU fall between 1.6 and 3.6 days per decade for all data sets while all other African regions show much higher SU trends ranging from near 4 days up to 7.5 days per decade. Despite differences in magnitude of change, the absolute threshold indices, SU and/or TR, show the highest decadal trends across NA, WA and EA regions. NA experiences the highest decadal trend with an increase in TR of 6.6, 7.8, 8.4 and 9 days per decade from BEST, MERRA2, JRA-55 and ERA5, respectively. WA shows a TR increase of 6 to 8.5 days from the reanalysis data sets and 2.2 days per decade from BEST. EA shows a TR increase of 4.5 to 7 days per decade from BEST, ERA5 and JRA-55 (and <4 days from MERRA2), while SA experienced an increase of <2 TR days per decade.

The best agreement among all data sets is observed for decadal trends of the 90th percentile index (TX90P) across all regions. The TX90P index shows an increase of about 1% to 4% per decade in all African regions. The minimum-temperature-based warm nights index

(WN) also consistently shows an increase of about 1.5 to 6 days per decade in all African regions. However, because of larger day-to-day variability, WN from the ERA5 data set shows the lowest decadal trend in all regions. WN from JRA-55 shows stronger decadal trend signals in all of the regions when compared with warm spell indices. Note that we do not interpret MERRA2 results in EA and WA due to the shortcomings discussed in Section 3.2.

The warm spell indices, WSDI_3 and WSDI_6, also show increasing trends. There, good agreement is found in all reanalysis data sets (mainly over NA and SA) showing an increase in the duration of warm spells by 1 to 4 days per decade. Warm spell indices from BEST observations (over NA and SA) show the highest decadal trends while JRA-55 shows the lowest trends in all inspected regions. Among all data sets, BEST shows the highest decadal trends over NA, WA and SA regions when the unreliable MERRA2 indices over WA are left aside. The highest difference between the observational BEST and the reanalysis data set is observed in TR over WA.

All regional trends of the analysed indices are found to be statistically significant ($\alpha = 0.05\%$ significance level) over the NA, WA and EA regions, except for SA where SU from MERRA2 is not significant.

Local-scale trends for several indices are presented in Figure 7, displaying SU, TR, TX90P and WSDI_6 from

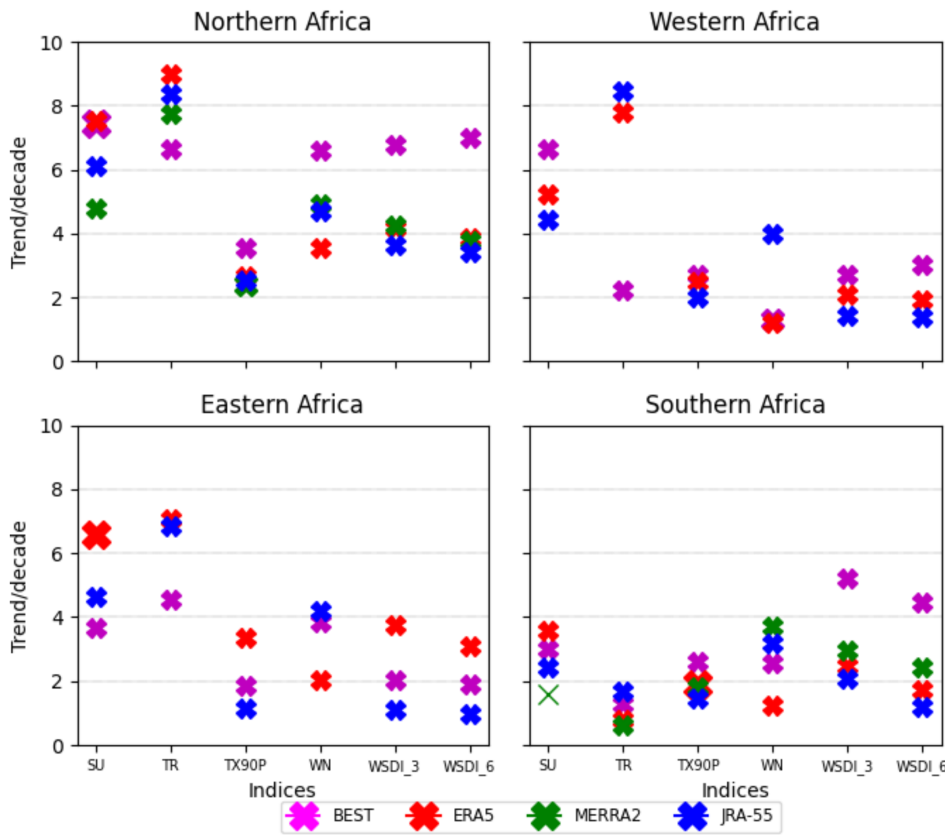


FIGURE 6 Decadal trends of extreme temperatures and heat wave indices (left to right in subpanels) SU and TR (days per decade), TX90P (% per decade), WN, WSDI_3 and WSDI_6 (days per decade), computed from BEST observations, ERA5, MERRA2 and JRA-55 reanalysis data sets over NA, WA, EA and SA regions. Bold shapes indicate statistically significant regional trends at significance level 0.05. Note that we do not show MERRA2 results in EA and WA regions due to their shortcomings discussed in Section 3.2 [Colour figure can be viewed at wileyonlinelibrary.com]

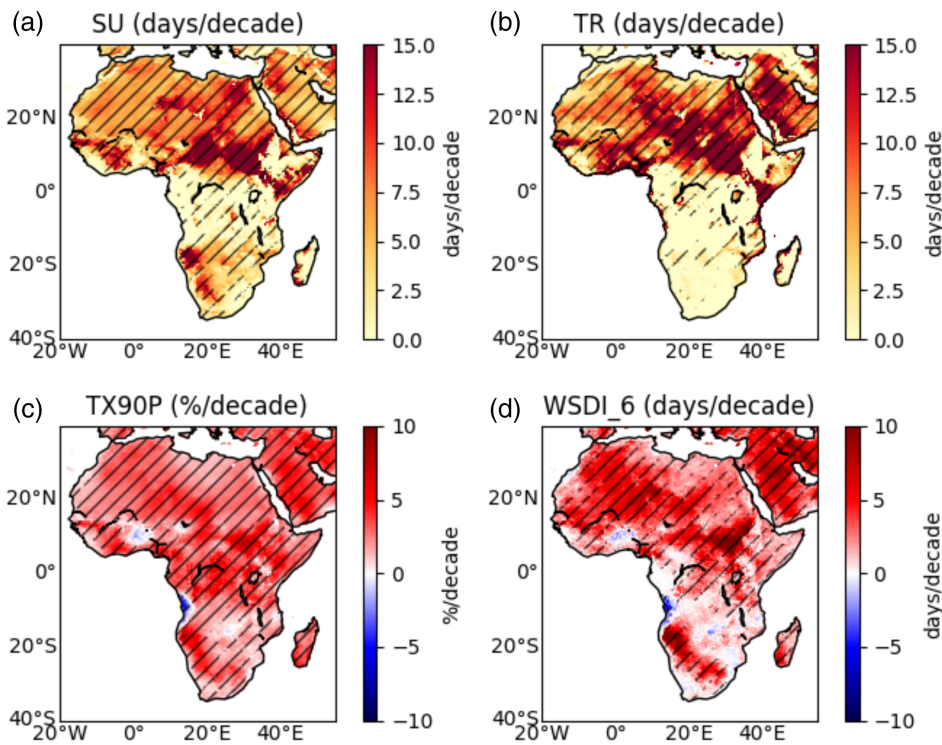


FIGURE 7 Spatial map of decadal trends (1980–2018) of (a) SU, (b) TR, (c) TX90P and (d) WSDI_6 computed from the ERA5 reanalysis data set. Hatching indicates a locally significant trend [Colour figure can be viewed at wileyonlinelibrary.com]

ERA5 at a resolution of $0.25^\circ \times 0.25^\circ$. Consistent with the results discussed above, we find the highest increase in heat wave days predominantly over NA and north of the equator (in parts of EA and WA) showing significant

trends. SU and TR show an increase of 5 to more than 10 days per decade, with relatively lower rates of change over the Ethiopian highlands in the EA region (Figure 7a,b). The SU index shows high decadal trends,

which are statistically significant also at regional scale over SA. TX90P shows statistically significant local-scale decadal trends over almost all of Africa (Figure 7c). The

heat wave index WSDI_6 also shows significant trends, except for SA where the six consecutive days criterion is too strict for this region.

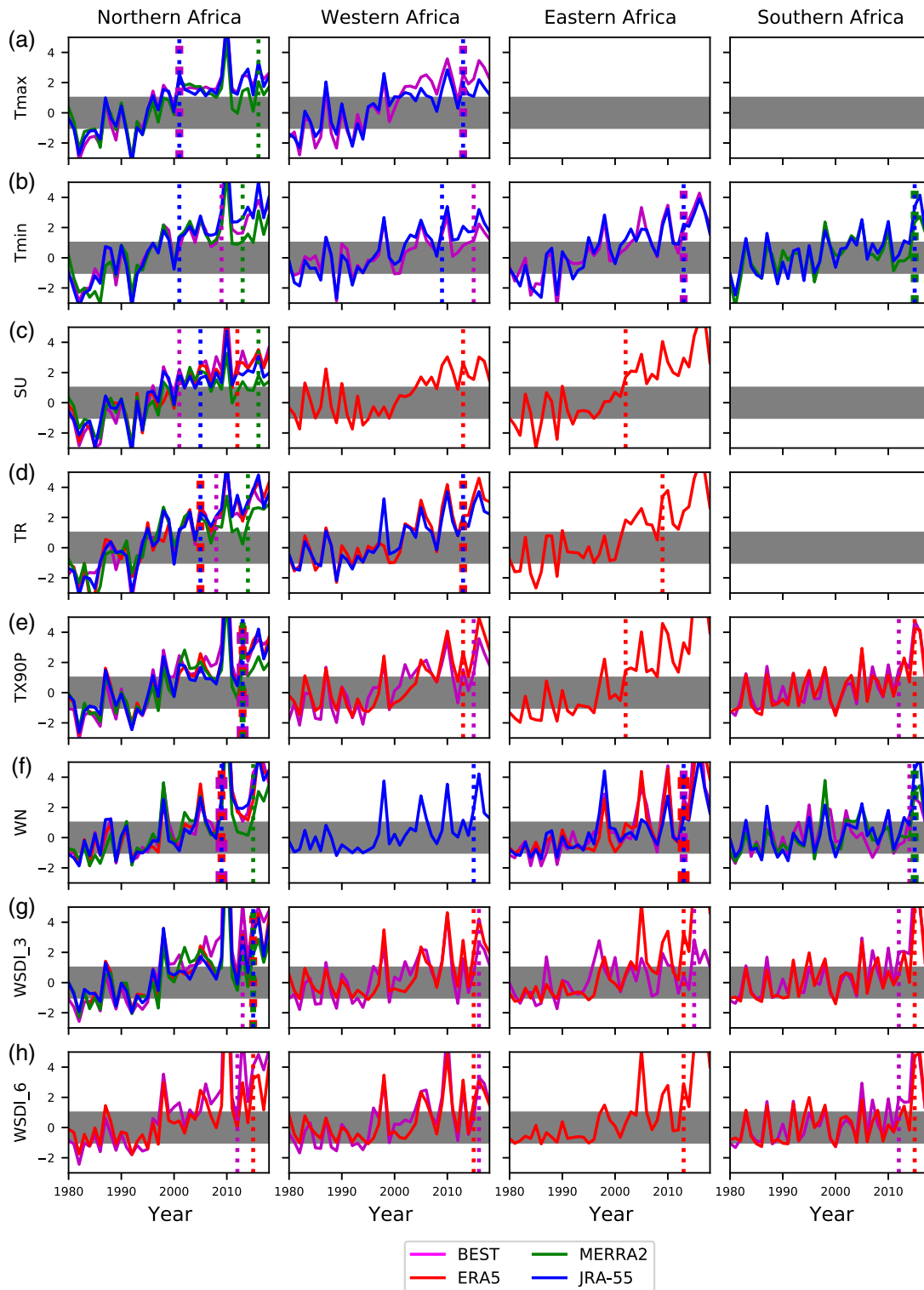


FIGURE 8 Time of emergence of trends over natural variability of (a,b) maximum and minimum temperature (T_{max} and T_{min}), (c,d) extreme temperature (SU, TR), and (e–h) heat wave indices (TX90P, WN, WSDI_3 and WSDI_6) shown for (left to right) the African regions NA, WA, EA and SA from observational (BEST) and reanalysis (ERA5, MERRA2 and JRA-55) data sets. Y-axis for all panels shows the S/N ratio. The shaded region between -1 and $+1$ shows the standard deviation of de-trended noise. Only emerged (continuously above the shaded region) trends are shown. Vertical lines show the year of emergence [Colour figure can be viewed at wileyonlinelibrary.com]

3.4 | Time of emergence (ToE) of heat waves

The ToE of heat wave trend signals over natural variability is presented in Figure 8. The earliest emergence is observed in the early 2000s, over NA for T_{\max} , T_{\min} and SU (from BEST and JRA-55) in 2001 and over EA for SU and TX90P (from ERA5) in 2002. In the NA region, emergence of trends in extreme temperature and heat wave days over the natural variability is observed in the past two decades for all indices and consistently in most data sets. Over the WA and EA regions, emergence of trends is found since about 2010 for most indices shown by at

least one or two data set(s) (except T_{\max} over EA). Also, over SA, emergence of trends is observed since 2010 but not for the full set of indices.

In general, trends of T_{\max} , T_{\min} and extreme temperature days (SU and TR) show earlier emergence while heat wave indices based on relative threshold and/or consecutive days (TX90P, WN, WSDI_3 and WSDI_6) show delayed emergence. Trend signals in the number of days with extreme temperatures show the earliest emergence over NA and EA regions. The minimum-temperature-based heat wave index WN shows emergence in all regions, though in WA from one data set only (JRA-55). Low variability in nighttime temperatures is regarded the main reason for the

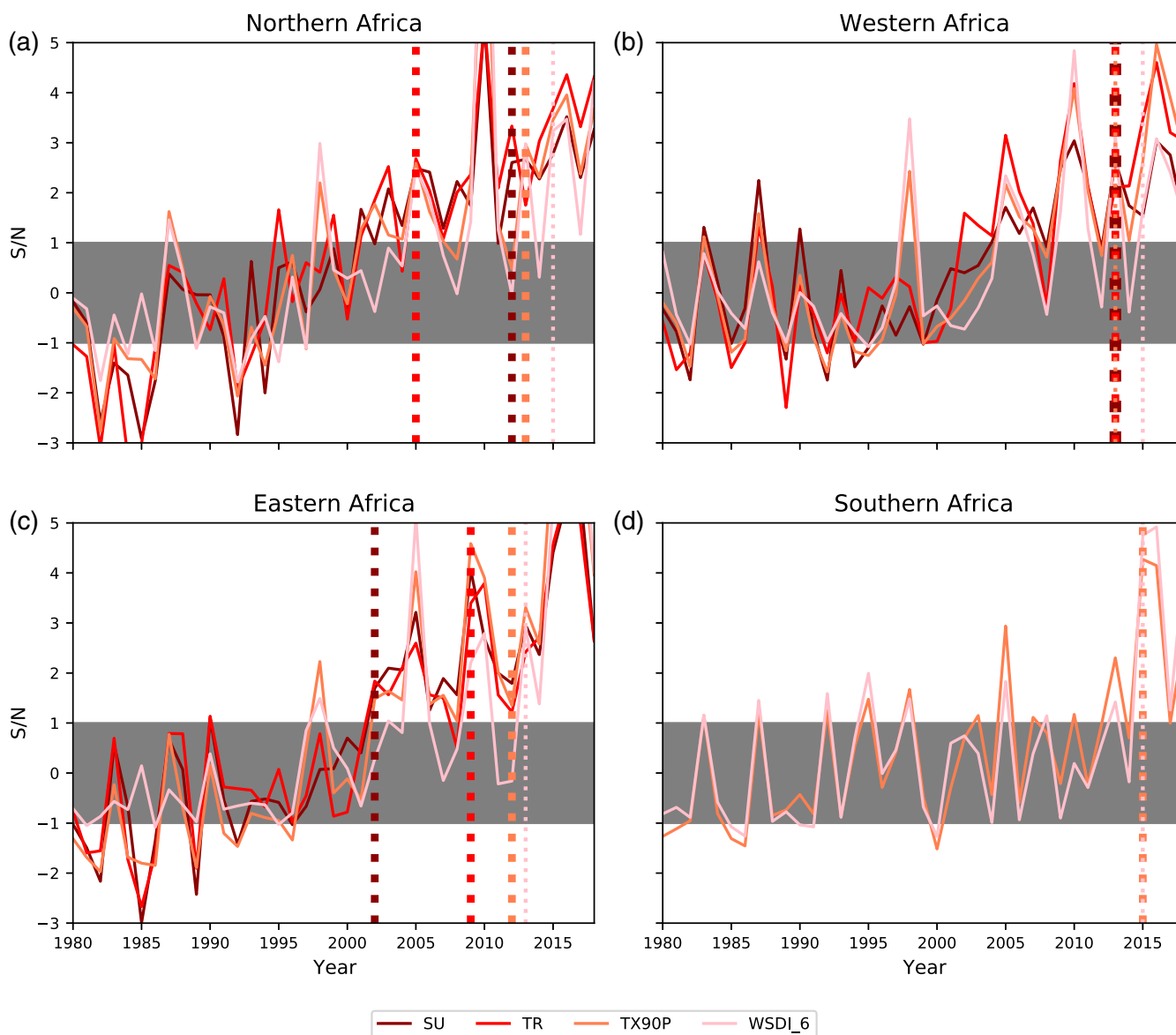


FIGURE 9 Comparison of standardized evolution of regional emerged heat wave for extreme temperatures (SU and TR) and heat wave indices (TX90P, WN, WSDI_3 and WSDI_6) shown for (a) NA, (b) WA, (c) EA and (d) SA regions from the ERA5 data set. The shaded region between -1 and $+1$ shows the standard deviation of de-trended noise. Vertical lines show the year of emergence. Only emerged (continuously above the shaded region) indices are shown [Colour figure can be viewed at wileyonlinelibrary.com]

early emergence of minimum-temperature-based indices (Morak et al., 2011, 2013; Bindoff et al., 2013). The later emergence of trends in heat waves indices WN, WSDI_3, WSDI_6 can be explained by the fact that these indices are based on more stringent persistence criteria. The number of heat wave days (WSDI_3 and WSDI_6) show emergence in the past decade in all African regions.

While BEST, JRA55 and ERA5 show emerging trends for a range of indices in several regions, indices computed from MERRA2 show emergence only over NA and SA regions but not over WA and EA. This is due to the unrealistic and high variability in MERRA2 during the period 2000–2010 (Gelaro et al., 2017) as discussed in Section 3.2. Consequently, the higher noise keeps the signal-to-noise ratio below one standard deviation.

Good agreement between all data sets is found for NA. All the data sets strikingly agree in identifying 2013 as year of emergence for TX90P index over NA. For some indices, for example, over WA and EA, only ERA5 shows emergence above the de-trended natural climate variability. However, other data sets are also near to emergence. They also would show emergence if there were no sharp declines in one of the recent years (e.g., TX90P and warm spell indices from JRA-55 over WA in 2018).

Due to the availability of reanalysis data, we can only use the recent period to characterize the initial heat wave activity. Thus, our ToE estimate is conservative (although the natural variability is de-trended) and may be later than a comparison with earlier time periods that would better represent the quasi-natural climate system. This may be the reason why some indices show no or delayed emergence over EA and SA regions.

The influence of absolute thresholds, or percentile thresholds and/or consecutive day criteria on ToE of heat wave indices from natural variability is demonstrated in Figure 9. SU, TR, TX90P and WSDI_6 from ERA5 are plotted for the four African regions. Because of stronger trend signals, the earliest ToE primarily comes from absolute threshold indices, SU and TR. Therefore, the earliest emergence of SU over NA can be explained by its strong trend signal. However, the time of emergence is delayed to the recent past for heat wave indices, which are based on relative thresholds (TX90P) and/or consecutive days (WSDI_6), the latter index requiring a longer duration of the extreme.

A study on the ToE based on climate models by King et al. (2015) showed that WA is the only region in Africa where temperature extremes would emerge prior to 2014. In their analysis, they assessed ToE of temperature extremes using model-based estimates of variability and 1860–1910 as reference period for representing natural climate variability. Our observation-based results, in contrast, show an earlier ToE of not only temperature extremes but also heat wave indices, and not only over

WA but also over NA, EA and SA regions of Africa. Even using conservative estimates of ToE, our observation-based analysis demonstrates that temperature extremes and heat waves have already emerged over the African region, and since the early 2000's.

4 | CONCLUSION

In this study, we assessed changes in temperature and heat waves over different regions of Africa using gridded observational (CRU, BEST) and state-of-the-art reanalysis (ERA5, MERRA2 and JRA-55) data sets. All data sets represent the seasonal cycle well and show increasing trends in monthly mean temperatures over all the investigated regions, Northern Africa (NA), Western Africa (WA), Eastern Africa (EA) and Southern Africa (SA). The data sets exhibit highest decadal temperature trends over NA and lowest decadal temperature trends over SA.

Extreme temperatures are rising and heat wave indices show an increase in heat wave occurrence over all of the African regions. Although the rates of increase differ between regions and the data sets, the detected trends are found to be statistically significant (except SU over SA, in MERRA2). Absolute threshold-based indices for extreme temperatures, summer days (SU) and tropical nights (TR), show the highest decadal trends in most of the African regions, compared to relative threshold indices, 90th percentile (TX90P), warm nights (WN), and warm spell duration indices (WSDI_3, WSDI_6).

In the period from 1980 to 2018 analysed in this study, an increase in TR of 2 to 9 days per decade was found in NA (all four data sets), WA (three data sets) and EA (two data sets) regions, with an increasing trend of <2 days per decade in SA. The SU trend ranges between 3.7 and 7.7 days per decade for all regions except for SA, where it is 1.8 to 3.8 days per decade. TX90P trends are 1% to 4% per decade and the warm spell duration index was found to increase by a maximum of 7 days per decade. The decadal trends of extreme temperature and heat wave days from all the observational and reanalysis data sets are statistically significant ($\alpha = 0.05\%$ significance level) over all regions of Africa except SU from MERRA2 over SA. In addition to regional mean changes, the heat wave indices also show statistically significant increasing trends at the local scale, based on ERA5.

Most analysed indices show the highest number of heat wave days in 2010 (over NA and WA), and 2016 (over EA and SA). Both observational and reanalysis data sets identify 2010 as a year of exceptional heat wave occurrence over NA, while 2016 is identified as the year of highest heat wave occurrence, relative to the remaining years analysed, over EA and SA.

Emergence of the trend signals from natural variability was found in all regions for most heat wave indices. Specifically, over NA, all indices consistently show emergence above the natural climate variability in the past two decades. The earliest time of emergence was found for T_{\max} and T_{\min} and related extreme temperature indices, SU and TR over NA and EA in the early 2000s. Trends in warm spell days emerge over natural variability in the past decade consistently in all African regions.

Even though the time of emergence estimate is conservative as the reference period 1980–2009 represents the quasi-natural climate system is in the recent years, the observations show that heat wave trend signals have already emerged over natural variability in all African regions, and that the emergence is qualitatively consistent across different heat wave metrics, supporting the result. Furthermore, our findings show earlier time of emergence of heat wave trend signals when basing emergence on observed variability and change compared to estimates from model studies, and in all the inspected regions of the African continent.

In general, trend signals of absolute-threshold based extreme temperatures show earlier time of emergence from natural variability than heat wave indices based on percentile and/or consecutive days (TX90P, WN and warm spell indices). Specifically, the minimum-temperature-based heat metric, WN, shows earlier emergence over NA and over EA compared to warm spell indices.

Despite differences in magnitudes, the increasing trend of temperature and heat wave indices show reasonable consistency in the data sets used in this study. Disregarding the shortcoming of MERRA2 over tropical regions in the period 2000–2010, the good overall agreement underpins the importance of analysing multiple data sets for gaining robust results. Furthermore, the consistency of observational and reanalysis data sets in identifying heat wave days is essential for further work on attributing the observed changes to anthropogenic climate change.

ACKNOWLEDGEMENTS


This study was funded by the Austrian Science Fund (FWF) under Research Grant W1256 (Doctoral Programme Climate Change: Uncertainties, Thresholds and Coping Strategies, <http://dk-climate-change.uni-graz.at>). Mastawesha Misganaw Engdaw's bench fee at University of Edinburgh was paid by the Sigrist foundation for the 6 months research visit, and GCH was also supported by NERC grant Emergence (NE/S004661/1). Mastawesha Misganaw Engdaw thanks GCH's research team at the School of Geosciences, University of Edinburgh, UK, for the fruitful discussions and support provided during the research visit. The authors acknowledge the Centre for Environmental Data Analysis (CEDA), the Berkeley

Earth Surface Temperature (BEST), the European Centre for Medium-Range Weather Forecasts (ECMWF), the National Oceanic Atmospheric Administration (NOAA) and the Japanese Meteorological Agency (JMA) for making CRU, BEST, ERA5, MERRA2 and JRA-55 data sets available online, respectively.

AUTHOR CONTRIBUTIONS

Mastawesha Engdaw: Conceptualization; formal analysis; investigation; methodology; visualization; writing - original draft; writing-review & editing. **Andrew Ballinger:** Methodology; supervision; writing-review & editing. **Gabi Hegerl:** Methodology; supervision; writing-review & editing. **Andrea Steiner:** Conceptualization; funding acquisition; methodology; resources; supervision; visualization; writing - original draft; writing-review & editing.

ORCID

Mastawesha Misganaw Engdaw  <https://orcid.org/0000-0001-8224-2369>

Andrew P. Ballinger  <https://orcid.org/0000-0003-3704-1976>

Gabriele C. Hegerl  <https://orcid.org/0000-0002-4159-1295>

Andrea K. Steiner  <https://orcid.org/0000-0003-1201-3303>

REFERENCES

- Barkhordarian, A., Bhend, J. and von Storch, H. (2012) Consistency of observed near surface temperature trends with climate change projections over the Mediterranean region. *Climate Dynamics*, 38(9–10), 1695–1702.
- Barkhordarian, A., von Storch, H. and Zorita, E. (2012) Anthropogenic forcing is a plausible explanation for the observed surface specific humidity trends over the Mediterranean area. *Geophysical Research Letters*, 39(19), 1–5.
- Bindoff, N.L., Stott, P.A., AchutaRao, K.M., Allen, M.R., Gillett, N., Gutzler, D., Hansingo, K., Hegerl, G., Hu, Y., Jain, S., Mokhov, I.I., Overland, J., Perlwitz, J., Sebbari, R. and Zhang, X. (2013) Detection and attribution of climate change: from global to regional. In: Stocker, T.F., Qin, D., Plattner, G.-K., Tignor, M., Allen, S.K., Boschung, J., Nauels, A., Xia, Y., Bex, V. and Midgley, P.M. (Eds.) *Climate Change 2013: The Physical Science Basis. Contribution of Working Group I to the Fifth Assessment Report of the Intergovernmental Panel on Climate Change*. Cambridge, United Kingdom and New York, NY, USA: Cambridge University Press.
- Ceccherini, G., Russo, S., Ameztoy, I., Marchese, A.F. and Carmona-Moreno, C. (2017) Heat waves in Africa 1981–2015, observations and reanalysis. *Natural Hazards and Earth System Sciences*, 17(1), 115–125. <https://doi.org/10.5194/nhess-17-115-2017>.
- Chapman, L., Azevedo, J.A. and Prieto-Lopez, T. (2013) Urban heat & critical infrastructure networks: a viewpoint. *Urban Climate*, 3, 7–12.

- Christidis, N. and Stott, P.A. (2016) Attribution analyses of temperature extremes using a set of 16 indices. *Weather and Climate Extremes*, 14, 24–35. <https://doi.org/10.1016/j.wace.2016.10.003>.
- Coumou, D. and Rahmstorf, S. (2012) A decade of weather extremes. *Nature Climate Change*, 2(7), 491–496. <https://doi.org/10.1038/nclimate1452>.
- Cowan, T., Purich, A., Perkins, S., Pezza, A., Boschat, G. and Sadler, K. (2014) More frequent, longer, and hotter heat waves for Australia in the twenty-first century. *Journal of Climate*, 27(15), 5851–5871. <https://doi.org/10.1175/JCLI-D-14-00092.1>.
- Diffenbaugh, N.S. and Scherer, M. (2011) Observational and model evidence of global emergence of permanent, unprecedented heat in the 20th and 21st centuries. *Climatic Change*, 107(3–4), 615–624. <https://doi.org/10.1007/s10584-011-0112-y>.
- Evan, A.T., Flamant, C., Lavaysse, C., Kocha, C. and Saci, A. (2015) Water vapor-forced greenhouse warming over the Sahara Desert and the recent recovery from the Sahelian drought. *Journal of Climate*, 28(1), 108–123. <https://doi.org/10.1175/JCLI-D-14-00039.1>.
- Field, C.B., Barros, V., Stocker, T.F. and Dahe, Q. (Eds.). (2012) *Managing the Risks of Extreme Events and Disasters to Advance Climate Change Adaptation: Special Report of the Intergovernmental Panel on Climate Change*. Cambridge, UK, and New York, NY, USA: Cambridge University Press.
- Gebrechorkos, S.H., Hülsmann, S. and Bernhofer, C. (2019) Changes in temperature and precipitation extremes in Ethiopia, Kenya, and Tanzania. *International Journal of Climatology*, 39(1), 18–30. <https://doi.org/10.1002/joc.5777>.
- Gelaro, R., McCarty, W., Suárez, M.J., Todling, R., Molod, A., Takacs, L., Randles, C.A., Darmenov, A., Bosilovich, M.G., Reichle, R. and Wargan, K. (2017) The modern-era retrospective analysis for research and applications, version 2 (MERRA-2). *Journal of Climate*, 30(14), 5419–5454. <https://doi.org/10.1175/JCLI-D-16-0758.1>.
- Guha-Sapir, D., Hargitt, D. and Hoyois, P. (2004) *Thirty Years of Natural Disasters 1974–2003: The Numbers*. Louvain-la-Neuve, Belgium: Presses Universities de Louvain.
- Guirguis, K., Gershunov, A., Tardy, A. and Basu, R. (2014) The impact of recent heat waves on human health in California. *Journal of Applied Meteorology and Climatology*, 53(1), 3–19. <https://doi.org/10.1175/JAMC-D-13-0130.1>.
- Guo, X., Huang, J., Luo, Y., Zhao, Z. and Xu, Y. (2017) Projection of heat waves over China for eight different global warming targets using 12 CMIP5 models. *Theoretical and Applied Climatology*, 128(3–4), 507–522. <https://doi.org/10.1007/s00704-015-1718-1>.
- Harrington, L.J., Frame, D.J., Fischer, E.M., Hawkins, E., Joshi, M. and Jones, C.D. (2016) Poorest countries experience earlier anthropogenic emergence of daily temperature extremes. *Environmental Research Letters*, 11(5), 055007. <https://doi.org/10.1088/1748-9326/11/5/055007>.
- Hawkins, E., Anderson, B., Diffenbaugh, N., Mahlstein, I., Betts, R., Hegerl, G., Joshi, M., Knutti, R., McNeall, D., Solomon, S. and Sutton, R. (2014) Uncertainties in the timing of unprecedented climates. *Nature*, 511(7507), E3–E5. <https://doi.org/10.1038/nature13523>.
- Hawkins, E. and Sutton, R. (2012) Time of emergence of climate signals. *Geophysical Research Letters*, 39(1), 1–6. <https://doi.org/10.1029/2011GL050087>.
- Hegerl, G.C., Hanlon, H. and Beierkuhnlein, C. (2011) Elusive extremes. *Nature Geoscience*, 4(3), 142–143. <https://doi.org/10.1038/ngeo1090>.
- Hersbach, H., Bell, B., Berrisford, P., Hirahara, S., Horányi, A., Muñoz-Sabater, J., Nicolas, J., Peubey, C., Radu, R., Schepers, D., Simmons, A., Soci, C., Abdalla, S., Abellan, X., Balsamo, G., Bechtold, P., Biavati, G., Bidlot, J., Bonavita, M., Chiara, G.D., Dahlgren, P., Dee, D., Diamantakis, M., Dragani, R., Flemming, J., Forbes, R., Fuentes, M., Geer, A., Haimberger, L., Healy, S., Hogan, R.J., Hólm, E., Janisková, M., Keeley, S., Laloyaux, P., Lopez, P., Lupu, C., Radnoti, G., de Rosnay, P., Rozum, I., Vamborg, F., Villaume, S. and Thépaut, J.-N. (2020) The ERA5 global reanalysis. *Quarterly Journal of the Royal Meteorological Society*, 146, 1999–2049. <https://doi.org/10.1002/qj.3803>.
- IPCC. (2014) *Climate change 2014: impacts, adaptation, and vulnerability. Part B: regional aspects*. In: Barros, V.R., Field, C.B., Dokken, D.J., Mastrandrea, M.D., Mach, K.J., Bilir, T.E., Chatterjee, M., Ebi, K.L., Estrada, Y.O., Genova, R.C., Girma, B., Kissel, E.S., Levy, A.N., MacCracken, S., Mastrandrea, P.R. and White, L.L. (Eds.) *Contribution of Working Group II to the Fifth Assessment Report of the Intergovernmental Panel on Climate Change*. Cambridge, United Kingdom and New York, NY, USA: Cambridge University Press, p. 688.
- King, A.D., Donat, M.G., Fischer, E.M., Hawkins, E., Alexander, L. V., Karoly, D.J., Dittus, A.J., Lewis, S.C. and Perkins, S.E. (2015) The timing of anthropogenic emergence in simulated climate extremes. *Environmental Research Letters*, 10(9), 094015. <https://doi.org/10.1088/1748-9326/10/9/094015>.
- King, A.D., Donat, M.G., Hawkins, E. and Karoly, D.J. (2017) Timing of anthropogenic emergence in climate extremes. *Climate Extremes: Patterns and Mechanisms*, 93–103. <https://doi.org/10.1002/9781119068020.ch6>.
- Kobayashi, S., Ota, Y., Harada, Y., Ebata, A., Moriya, M., Onoda, H., Onogi, K., Kamahori, H., Kobayashi, C., Endo, H. and Miyaoka, K. (2015) The JRA-55 reanalysis: general specifications and basic characteristics. *Journal of the Meteorological Society of Japan. Series. II*, 93(1), 5–48. <https://doi.org/10.2151/jmsj.2015-001>.
- Kuglitsch, F.G., Toreti, A., Xoplaki, E., Della-Marta, P.M., Zerefos, C.S., Türkeş, M. and Luterbacher, J. (2010) Heat wave changes in the eastern mediterranean since 1960. *Geophysical Research Letters*, 37(4), 1–5. <https://doi.org/10.1029/2009GL041841>.
- Largerou, Y., Guichard, F., Roehrig, R., Couvreur, F. and Barbier, J. (2020) The April 2010 north African heatwave: when the water vapor greenhouse effect drives nighttime temperatures. *Climate Dynamics*, 54(9), 3879–3905. <https://doi.org/10.1007/s00382-020-05204-7>.
- Lau, W.K. and Kim, K.M. (2012) The 2010 Pakistan flood and Russian heat wave: Teleconnection of hydrometeorological extremes. *Journal of Hydrometeorology*, 13(1), 392–403. <https://doi.org/10.1175/JHM-D-11-016.1>.
- Lehner, F., Deser, C. and Terray, L. (2017) Toward a new estimate of “time of emergence” of anthropogenic warming: insights from dynamical adjustment and a large initial-condition model ensemble. *Journal of Climate*, 30(19), 7739–7756. <https://doi.org/10.1175/JCLI-D-16-0792.1>.

- Li, D., Yuan, J. and Kopp, R.B. (2020) Escalating global exposure to compound heat-humidity extremes with warming. *Environmental Research Letters*, 15, 1–11. <https://doi.org/10.1088/1748-9326/ab7d04>.
- Liao, W., Liu, X., Li, D., Luo, M., Wang, D., Wang, S., Baldwin, J., Lin, L., Li, X., Feng, K. and Hubacek, K. (2018) Stronger contributions of urbanization to heat wave trends in wet climates. *Geophysical Research Letters*, 45(20), 11–310. <https://doi.org/10.1029/2018GL079679>.
- Lobell, D.B., Torney, A. and Field, C.B. (2011) Climate extremes in California agriculture. *Climatic Change*, 109(1), 355–363.
- Mahlstein, I., Knutti, R., Solomon, S. and Portmann, R.W. (2011) Early onset of significant local warming in low latitude countries. *Environmental Research Letters*, 6(3), 034009.
- Masood, I., Majid, Z., Sohail, S., Zia, A. and Raza, S. (2015) The deadly heat wave of Pakistan, June 2015. *Indian Journal of Occupational and Environmental Medicine*, 6(4 October), 672–247.
- Morak, S., Hegerl, G.C. and Christidis, N. (2013) Detectable changes in the frequency of temperature extremes. *Journal of Climate*, 26, 1561–1574.
- Morak, S., Hegerl, G.C. and Kenyon, J. (2011) Detectable regional changes in the number of warm nights. *Geophysical Research Letters*, 38, L17703.
- Moron, V., Oueslati, B., Pohl, B., Rome, S. and Janicot, S. (2016) Trends of mean temperatures and warm extremes in northern tropical Africa (1961–2014) from observed and PPCA-reconstructed time series. *Journal of Geophysical Research: Atmospheres*, 121(10), 5298–5319. <https://doi.org/10.1002/2015JD024303>.
- Munich Re. (2011). TOPICS GEO, natural catastrophes 2010, analyses, assessments. Positions.
- Nicholson, S.E., Nash, D.J., Chase, B.M., Grab, S.W., Shanahan, T. M., Verschuren, D., Asrat, A., Lézine, A.M. and Umer, M. (2013) Temperature variability over Africa during the last 2000 years. *The Holocene*, 23(8), 1085–1094. <https://doi.org/10.1177/0959683613483618>.
- Oueslati, B., Pohl, B., Moron, V., Rome, S. and Janicot, S. (2017) Characterization of heat waves in the Sahel and associated physical mechanisms. *Journal of Climate*, 30(9), 3095–3115. <https://doi.org/10.1175/JCLI-D-16-0432.1>.
- Parkes, B., Cronin, J., Dessens, O. and Sultan, B. (2019) Climate change in Africa: costs of mitigating heat stress. *Climatic Change*, 154, 1–16. <https://doi.org/10.1007/s10584-019-02405-w>.
- Perkins, S.E. (2015) A review on the scientific understanding of heatwaves—their measurement, driving mechanisms, and changes at the global scale. *Atmospheric Research*, 164, 242–267. <https://doi.org/10.1016/j.atmosres.2015.05.014>.
- Ratnam, J.V., Behera, S.K., Ratna, S.B., Rajeevan, M. and Yamagata, T. (2016) Anatomy of Indian heatwaves. *Scientific Reports*, 6, 24395. <https://doi.org/10.1038/srep24395>.
- Robine, J.M., Cheung, S.L.K., Le Roy, S., Van Oyen, H., Griffiths, C., Michel, J.P. and Herrmann, F.R. (2008) Death toll exceeded 70,000 in Europe during the summer of 2003. *Comptes Rendus Biologies*, 331(2), 171–178. <https://doi.org/10.1016/j.crvi.2007.12.001>.
- Rohini, P., Rajeevan, M. and Srivastava, A.K. (2016) On the variability and increasing trends of heat waves over India. *Scientific Reports*, 6, 26153. <https://doi.org/10.1038/srep26153>.
- Russo, S., Marchese, A.F., Sillmann, J. and Immé, G. (2016) When will unusual heat waves become normal in a warming Africa? *Environmental Research Letters*, 11(5), 054016. <https://doi.org/10.1088/1748-9326/11/5/054016>.
- Russo, S., Sillmann, J. and Sterl, A. (2017) Humid heat waves at different warming levels. *Scientific Reports*, 7(1), 1–7. <https://doi.org/10.1038/s41598-017-07536-7>.
- Seneviratne, S.I., Nicholls, N., Easterling, D., Goodess, C.M., Kanae, S., Kossin, J., et al. (2012) Changes in climate extremes and their impacts on the natural physical environment. In: *Managing the Risks of Extreme Events and Disasters to Advance Climate Change Adaptation: Special Report of the Intergovernmental Panel on Climate Change*. Cambridge, UK, and New York, NY, USA: Cambridge University Press, pp. 109–230.
- Shafiei Shiva, J., Chandler, D.G. and Kunke, K.E. (2019) Localized changes in heat wave properties across the United States. *Earth's Future*, 7(3), 300–319. <https://doi.org/10.1029/2018EF001085>.
- Sherwood, S.C. (2018) How important is humidity in heat stress? *Journal of Geophysical Research: Atmospheres*, 123(21), 11–808. <https://doi.org/10.1029/2018JD028969>.
- Smith, T.T., Zaitchik, B.F. and Gohlke, J.M. (2013) Heat waves in the United States: definitions, patterns and trends. *Climatic Change*, 118(3–4), 811–825. <https://doi.org/10.1007/s10584-012-0659-2>.
- The World Bank Group. 2020. Access to electricity (% of population). <https://data.worldbank.org/indicator/EG.ELC.ACCS.ZS?locations=ZG&view=chart>
- Vizy, E.K. and Cook, K.H. (2012) Mid-twenty-first-century changes in extreme events over northern and tropical Africa. *Journal of Climate*, 25(17), 5748–5767. <https://doi.org/10.1175/JCLI-D-11-00693.1>.
- Wang, P., Tang, J., Sun, X., Liu, J. and Juan, F. (2019) Spatiotemporal characteristics of heat waves over China in regional climate simulations within the CORDEX-EA project. *Climate Dynamics*, 52(1–2), 799–818. <https://doi.org/10.1007/s00382-018-4167-6>.
- Zhang, X., Hegerl, G., Zwiers, F.W. and Kenyon, J. (2005) Avoiding inhomogeneity in percentile-based indices of temperature extremes. *Journal of Climate*, 18(11), 1641–1651. <https://doi.org/10.1175/JCLI3366.1>.

How to cite this article: Engdaw, M. M., Ballinger, A. P., Hegerl, G. C., & Steiner, A. K. (2022). Changes in temperature and heat waves over Africa using observational and reanalysis data sets. *International Journal of Climatology*, 42(2), 1165–1180. <https://doi.org/10.1002/joc.7295>